

ONLINE SIMULTANEOUS STATE ESTIMATION AND PARAMETER ADAPTATION FOR BUILDING PREDICTIVE CONTROL

Mehdi Maasoumy*
Department of Mechanical Engineering
University of California
Berkeley, California 94720-1740
Email: mehdi@me.berkeley.edu

Barzin Moridian
Meysam Razmara
Mahdi Shahbakhti
Mechanical Engineering-Engineering Mechanics Department
Michigan Technological University
Houghton, Michigan 49931-1295
Emails: bmoridia, mrazmara, mahdish@mtu.edu

Alberto Sangiovanni-Vincentelli
Department of Electrical Engineering and Computer Sciences
University of California
Berkeley, California 94720-1770
Email: alberto@eecs.berkeley.edu

ABSTRACT

Model-based control of building energy offers an attractive way to minimize energy consumption in buildings. Model-based controllers require mathematical models that can accurately predict the behavior of the system. For buildings, specifically, these models are difficult to obtain due to highly time varying, and nonlinear nature of building dynamics. Also, model-based controllers often need information of all states, while not all the states of a building model are measurable. In addition, it is challenging to accurately estimate building model parameters (e.g. convective heat transfer coefficient of varying outside air). In this paper, we propose a modeling framework for “*on-line estimation*” of states and unknown parameters of buildings, leading to the Parameter-Adaptive Building (PAB) model. Extended Kalman filter (EKF) and unscented Kalman filter (UKF) techniques are used to design the PAB model which simultaneously tunes the parameters of the model and provides an estimate for all states of the model. The proposed PAB model is tested against experimental data collected from Lakeshore Center building at Michigan Tech University. Our results indicate that the new framework can accurately predict states and parameters of the building thermal model.

NOMENCLATURE

$\alpha_{i,j}$	Absorption coefficient of the wall between room i & j (-)
A_{w_i}	Area of the i^{th} wall (m^2)
A_{win_i}	Total area of window on walls surrounding i^{th} room (m^2)
C	Cloud coverage constant (-)
C_i^r	Heat capacity of the i^{th} room (kJ/ K)
$C_{i,j}^w$	Heat capacity of wall between room i & j (kJ/ K)
c_a	Specific heat capacity of air (kJ/ kg. K)
c_w	Specific heat capacity of wall material
ϵ	Emissivity coefficient (-)
h_{in}	Inside convection heat coefficient ($W/m^2.K$)
h_{out}	Outside convection heat coefficient ($W/m^2.K$)
IAQ	Internal Air Quality (-)
K	Cloud height coefficient (-)
k_w	Conductive heat transfer coefficient
L_w	Thickness of walls
\dot{m}_{r_i}	Air mass flow rate into the i^{th} room (kg/s)
$\mathcal{N}_{w_{i,j}}$	Set of all of neighboring nodes to node $w_{i,j}$ (-)
\mathcal{N}_i	Set of all of neighboring nodes to node i (-)
Q_{rad_i}	Radiative heat flux density on node i (W/m^2)
Q_{bldg}	Heat flow from the building to the environment (W/m^2)
Q_{sky}	Heat flow from the sky to the building (W/m^2)
Q_{solar}	Solar heat flow to the building (W/m^2)

*Address all correspondence to this author.

\dot{Q}_{int_i}	Internal heat generation in room i (W)
$R_{i,jk}$	Total thermal resistance between centerline of wall i & j and the side of wall where node k is located (K/ W)
$R_{i,j}^{win}$	Thermal resistance of window between room i & j (K/W)
RH	Relative humidity (-)
ψ	CO_2 concentration in the room (ppm)
σ	Stefan-Boltzmann law constant ($W/m^2.K^4$)
τ_{w_i}	Transmissivity of glass of window i (-)
T_{bldg}	Average temperature of the building ($^{\circ}C$)
T_{r_i}	Temperature of the i^{th} room ($^{\circ}C$)
T_{out}	Outside air temperature ($^{\circ}C$)
$T_{w_i,j}$	Temperature of the wall between room i & j ($^{\circ}C$)
T_{s_i}	Supply air temperature of the i^{th} room ($^{\circ}C$)

1 Introduction

Total primary energy consumption in the United States increased from 78.3 quads in 1980 to over 100 quads in 2008, of which the building sector accounts for about 40% [1]. The building sector is also responsible for almost 40% of greenhouse gas emissions and 70% of electricity use. About 50% of “site” energy consumption in buildings is directly related to space heating, cooling and ventilation [1]. Therefore, reducing the energy consumption of buildings by designing smart control systems to operate the heating, ventilation and air conditioning (HVAC) system in a more efficient way is critically important to address energy and environmental concerns in the United States and worldwide.

Buildings are dynamical systems with uncertain and time-varying plant and occupant characteristics. The heat transfer characteristics of a building are highly dependent on the ambient conditions. For instance, heat transfer properties such as convective heat transfer coefficient h , of peripheral walls is dependent on outside temperature, wind speed and direction. Also, unmodelled dynamics of a building¹ is function of 1) *external factors*: ambient weather conditions such as radiative heat flux into the walls and windows, and cloudiness of the sky, and 2) *internal factors*: such as occupancy level, internal heat generation from lighting, and computers. These quantities are highly time-varying and therefore the dynamics of the building and, consequently, parameters of the mathematical model describing the dynamics of the buildings are constantly changing with time. Accordingly, the estimation algorithms utilized to identify these parameters should take the *time-varying* aspect of buildings into account and be *adaptive* in this respect.

Reliable dynamical models are crucial to model predictive control strategies. Modeling and system identification are the most challenging and time-consuming parts of building predictive control [3]. To address this challenge, over the last few years numerous mathematical models of building thermal dynamics have been proposed in the literature. Resistor-capacitor (RC) models with disturbances to capture unmodelled dynamics have

been proposed in [2, 4, 5]. A bilinear version of an RC model is presented in [6] that takes into account weather predictions to increase building energy efficiency. In [7], the authors found that time varying properties such as occupancy can significantly change the dynamic thermal model and influence how building models are identified. While modeling a multi-zone building, the authors observed that the experimental data often did not have sufficient quality for system identification and hence, proposed a closed-loop architecture for active system identification using prediction-error identification method (PEM). Other modeling techniques with application in building predictive control include: *subspace methods*, *MPC relevant identification (MRI)*, *deterministic semi-physical modeling (DSPM)*, and *probabilistic semi-physical modeling (PSPM)*. In this paper we focus on DSPM.

Building models can be linear or nonlinear. While nonlinear models typically provide better prediction of building thermal dynamics, they are computationally intensive when incorporated in building controller algorithms. On the other hand, linear models are less computationally intensive for use in building controllers but they are limited to the operating zones they have been tuned for. One approach to increase the accuracy of the linear building models is to use an adaptive parameter estimation technique such that the building parameters are updated as the environment changes. This leads to an adaptive modeling framework for building predictive control. Although this technique has been adopted for simultaneous state-parameter estimation in other applications [8–10], to the best of the authors’ knowledge, this paper is the first study on developing adaptive modeling framework for simultaneous estimation of building *parameter, states and unmodelled dynamics*.

The contributions of this paper are two: a novel adaptive modeling framework for building predictive control and the application of extended Kalman filter (EKF) and unscented Kalman filter (UKF) techniques for building on-line parameter identification and state estimation using historical data from a test bed.

The remainder of the paper is organized as follows. A physics driven building model based on [4] is described in Section 2 and a new building model is developed based on the test bed in this work. Section 3 explains combined state-parameter estimation algorithms including EKF and UKF. The experimental set-up for collecting building historical data is detailed in Section 4. Performance of the designed adaptive building modeling framework is tested in Section 5 by comparing measured and estimated room temperatures. Finally, the summary and conclusions are presented in Section 6.

2 Mathematical Model

Fig. 1 depicts the schematic of a typical room which will be studied. We use lumped model analysis to reduce the complexity, and obtain a low order model, suitable for control purposes. Note that due to having forced convection inside the room, the temperature is assumed uniform inside the room. We use the RC

¹See [2].

model from [5] in which the building is considered as a network. Then we modify the representation of the system dynamics to account for *time varying* parameters by *augmenting* the parameters into the state vector.

2.1 Conductive and Convective Heat Transfer

There are two types of nodes in the building network: walls and rooms. There are in total n nodes, m of which represent rooms and the remaining $n - m$ nodes represent walls. We assign a number $i = 1, \dots, m$ to each room, and denote the temperature of the room with T_{r_i} . The wall node and temperature of the wall between room i and j is denoted by (i, j) and $T_{w_{i,j}}$, respectively, and is governed by the following equation:

$$C_{i,j}^w \frac{dT_{w_{i,j}}}{dt} = \sum_{k \in \mathcal{N}_{w_{i,j}}} \frac{T_{r_k} - T_{w_{i,j}}}{R_{i,j,k}} + r_{i,j} \alpha_{i,j} A_{w_{i,j}} Q_{rad_{i,j}} \quad (1)$$

where $C_{i,j}^w$, $\alpha_{i,j}$ and $A_{w_{i,j}}$ are heat capacity, radiation heat absorption coefficient and area of wall between room i and j , respectively. $R_{i,j,k}$ is the total thermal resistance between the centerline of wall (i, j) and the side of the wall where node k is located. $Q_{rad_{i,j}}$ is the radiative heat flux density on wall (i, j) . $\mathcal{N}_{w_{i,j}}$ is the set of all of neighboring nodes to node $w_{i,j}$. $r_{i,j}$ is equal to 0 for internal walls, and equal to 1 for peripheral walls (*i.e.* either i or j is the outside node). Temperature of the i^{th} room is governed by the following equation:

$$C_i^r \frac{dT_{r_i}}{dt} = \sum_{k \in \mathcal{N}_{r_i}} \frac{T_k - T_{r_i}}{R_{i,k}} + \dot{m}_{r_i} c_a (T_{s_i} - T_{r_i}) + w_i \tau_{w_i} A_{win_i} Q_{rad_i} + \dot{Q}_{int_i} \quad (2)$$

where T_{r_i} , C_i^r and \dot{m}_{r_i} are the temperature, heat capacity and air mass flow into the room i , respectively. c_a is the specific heat capacity of air. T_{s_i} is the temperature of the supply air to room i . w_i is equal to 0 if none of the walls surrounding room i have window, and is equal to 1 if at least one of them has a window. τ_{w_i} is the transmissivity of glass of window i , A_{win_i} is the total area of window on walls surrounding room i , Q_{rad_i} is the radiative heat flux density per unit area radiated to room i , and \dot{Q}_{int_i} is the internal heat generation in room i . \mathcal{N}_{r_i} is the set of all of the neighboring "room" nodes to room i . The details of building thermal modeling and estimation of the unmodelled dynamics is available in [2, 4, 5]. Note that we approximate the values of $Q_{rad_i}(t)$ and $\dot{Q}_{int_i}(t)$ based on the following equations:

$$Q_{rad_i}(t) = \tau T_{out}(t) + \zeta \quad (3)$$

$$\dot{Q}_{int_i}(t) = \mu \Psi(t) + v \quad (4)$$

where T_{out} and Ψ are the outside air temperature and CO_2 concentration in the room, respectively. Parameters τ , ζ , μ and v are obtained by the parameter estimation algorithm detailed in Section 3.

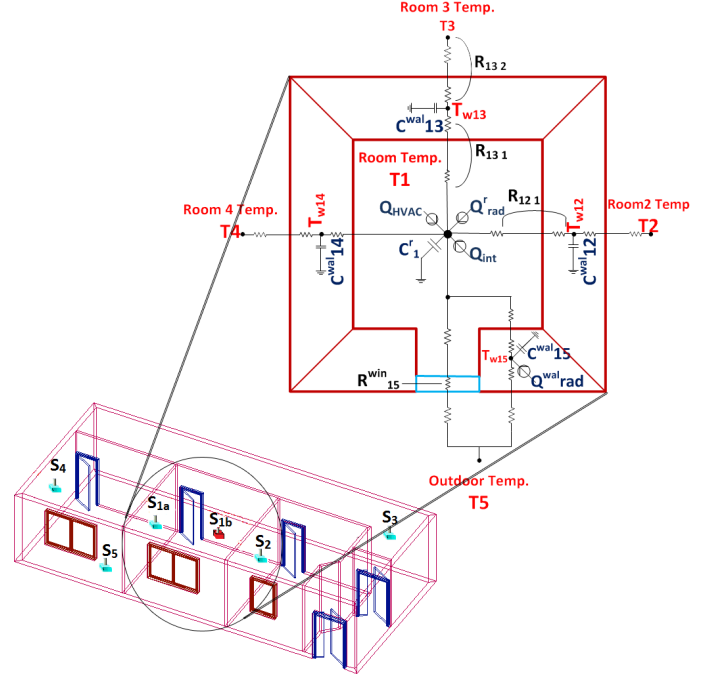


Figure 1. Schematic of a typical room with a window. Temperature sensors are denoted by "S" in this figure.

2.2 Radiative Heat Transfer

We compute the radiative heat transfer between building and ambient environment as proposed in [11]. The amount of heat transferred from the building to the environment is given by the Stefan-Boltzmann law:

$$Q_{bldg} = \epsilon \sigma T_{bldg}^4 \quad (5)$$

where T_{bldg} is the average temperature of the building.

We also consider solar radiation heat transfer, Q_{solar} emitted on the walls, and inside the room through the windows. The data used in this paper is based on the past 30 years monthly average of solar radiation for flat-plate collectors facing south (resembling the south facing flat vertical walls of the building), and is obtained from NREL (National Renewable Energy Laboratory) [12] database for Houghton, MI in January.

Furthermore, we take into account the radiation cooling at night (*i.e.* sky thermal radiation to the building) based on the proposed relation in [11]:

$$Q_{sky} = (1 + KC^2) 8.78 \times 10^{-13} T_{out}^{5.852} RH^{0.07195} \quad (6)$$

where K is the coefficient related to the cloud height and C is a function of cloud coverage. We use $K = 0.34$ and $C = 0.8$ for simulations, as explained in [11]. T_{out} is the outside air temperature, and RH is the air relative humidity percentage.

The total radiation exchange between building and ambient environment is then given by:

$$Q_{rad} = Q_{sky} + Q_{solar} - Q_{bldg} \quad (7)$$

Note that Q_{sky} and Q_{solar} are heat flow *into* the building, and Q_{bldg} , is the heat flow *from* the building *to* the environment.

The heat transfer equations for each wall and room yield the following system dynamics:

$$\begin{aligned} \dot{x}_t &= f(x_t, u_t, d_t, t) \\ y_t &= Cx_t \end{aligned} \quad (8)$$

where $x_t \in \mathbb{R}^n$ is the state vector representing the temperature of the nodes in the thermal network, $u_t \in \mathbb{R}^{lm}$ is the input vector representing the air mass flow rate and discharge air temperature of conditioned air into each thermal zone, and $y_t \in \mathbb{R}^m$ is the output vector of the system which represents the temperature of the thermal zones. l is the number of inputs to each thermal zone (e.g., air mass flow and supply air temperature). C is a matrix of proper dimension and the disturbance vector is given by $d_t = g(Q_{rad_i}(t), \dot{Q}_{int}(t), T_{out}(t))$.

2.3 Disturbance

Following the intuitive linear relation between T_{out} , \dot{Q}_{int} and Q_{rad} , we approximate g with an affine function of these quantities, leading to:

$$d_t = aQ_{rad_i}(t) + b\dot{Q}_{int}(t) + cT_{out}(t) + e \quad (9)$$

where e is a constant to be estimated. By substituting (3) and (4) into (9) and rearranging the terms, we get:

$$\begin{aligned} d_t &= (a\tau + c)T_{out}(t) + b\mu\Psi(t) + a\zeta + bv + e \\ &= \bar{a}T_{out}(t) + \bar{b}\Psi(t) + \bar{e} \end{aligned} \quad (10)$$

where $\bar{a} = a\tau + c$, $\bar{b} = b\mu$, and $\bar{e} = a\zeta + bv + e$. Therefore, only measurements of outside air temperature and CO_2 concentration level are needed to determine the disturbance. The values of \bar{a} , \bar{b} , and \bar{e} are estimated along with other parameters of the model.

2.4 State-Parameter Estimation

State space form of the system is required for state-parameter estimation. Here, the state space form of building equations is presented, using (1) for each wall and (2) for each room node in the building network.

$$\begin{aligned} \dot{x}_1 &= \frac{1}{C_1^w} \cdot \left(\left(\frac{1}{R_{12_1}} - \frac{1}{R_{13_1}} - \frac{1}{R_{14_1}} - \frac{1}{R_{15_1}} - \frac{1}{R_{15_1}^{win}} - \dot{m}_{r1}c_a \right) x_1 \right. \\ &\quad + \frac{x_2}{R_{12_1}} + \frac{x_3}{R_{13_1}} + \frac{x_4}{R_{14_1}} + \frac{x_5}{R_{15_1}} + c_a T_{s1} \dot{m}_{r1} \\ &\quad \left. + \frac{T_5}{R_{15_1}^{win}} + A_{win} \tau Q_{rad} + \dot{Q}_{int_1} \right) \end{aligned} \quad (11a)$$

$$\dot{x}_2 = \frac{1}{C_{21}^w} \cdot \left(\frac{x_1}{R_{21_1}} - \left(\frac{1}{R_{21_1}} + \frac{1}{R_{21_2}} \right) x_2 + \frac{T_2}{R_{21_2}} \right) \quad (11b)$$

$$\dot{x}_3 = \frac{1}{C_{31}^w} \cdot \left(\frac{x_1}{R_{31_1}} - \left(\frac{1}{R_{31_1}} + \frac{1}{R_{31_3}} \right) x_3 + \frac{T_3}{R_{31_3}} \right) \quad (11c)$$

$$\dot{x}_4 = \frac{1}{C_{41}^w} \cdot \left(\frac{x_1}{R_{41_1}} - \left(\frac{1}{R_{41_1}} + \frac{1}{R_{41_4}} \right) x_4 + \frac{T_4}{R_{41_4}} \right) \quad (11d)$$

$$\dot{x}_5 = \frac{1}{C_{51}^w} \cdot \left(\frac{x_1}{R_{51_1}} - \left(\frac{1}{R_{51_1}} + \frac{1}{R_{51_5}} \right) x_5 + \frac{T_5}{R_{51_5}} + A_{w51} \alpha Q_{rad} \right) \quad (11e)$$

where T_2, T_3, T_4, T_5 are the temperatures of the surrounding zones, as shown in Fig. 1. These temperatures act as disturbance to the system dynamics for a single zone thermal model, and x is the state vector:

$$x = [T_{r1}, T_{w12}, T_{w13}, T_{w14}, T_{w15}]^T \quad (12)$$

One way to adapt the model to account for time varying parameters is to assume that all the parameters of the model are independent, and hence define a state corresponding to each state. However, this would lead to excessive number of states. We take a different approach. Note that thermal properties of wall material (e.g. specific heat capacity and conductive heat transfer coefficient) are the same across the building. In addition, the thickness of internal walls and thickness of peripheral walls are the same throughout the building. Thus, we can reduce the number of independent parameters from 18 to 10. Hence we re-write the thermal equations of the wall, *i.e.* (11b)-(11d) as follows:

$$\dot{x}_2 = \frac{x_1}{C^w R^w} - \frac{2}{C^w R^w} x_2 + \frac{T_2}{C^w R^w} \quad (13)$$

$$\dot{x}_3 = \frac{x_1}{C^w R^w} - \frac{2}{C^w R^w} x_3 + \frac{T_3}{C^w R^w} \quad (14)$$

$$\dot{x}_4 = \frac{x_1}{C^w R^w} - \frac{2}{C^w R^w} x_4 + \frac{T_4}{C^w R^w} \quad (15)$$

$$\begin{aligned} \dot{x}_5 &= \frac{x_1}{C_{51}^w R_{51_1}} - \left(\frac{1}{C_{51}^w R_{51_1}} + \frac{1}{C_{51}^w R_{51_5}} \right) x_5 + \frac{T_5}{C_{51}^w R_{51_5}} \\ &\quad + \frac{A_{w51} \alpha Q_{rad}}{C_{51}^w} \end{aligned} \quad (16)$$

As shown in (17), $C_w R_w$ is not a function of the area of each

wall:

$$C^w R_w = (c_w A_w L_w) \left(\frac{L_w/2}{k_w A_w} + \frac{1}{h_{in} A_w} \right) = \frac{c_w L_w^2}{2k_w} + \frac{c_w L_w}{h_{in}} \quad (17)$$

where c_w , k_w , A_w and L_w are the specific heat capacity, conductive heat transfer coefficient of wall material, area and thickness of wall, respectively, and h_{in} is the indoor convective heat transfer coefficient. Hence, we can use one common term to express thermal capacitance-resistance between centerline of each wall and the node on each side of the wall for the equations of walls in the building.

In order to use Kalman filtering for parameter estimation along with state estimation we augment the parameter vector into state vector and define the new state update equation accordingly. Effectively, we augment the following *time-varying* parameters to the state vector:

$$x_6 = \frac{1}{C_1^r R_{12_1}} \quad x_7 = \frac{1}{C_1^r R_{13_1}} \quad (18)$$

$$x_8 = \frac{1}{C_1^r R_{14_1}} \quad x_9 = \frac{1}{C_1^r R_{15_1}} \quad (19)$$

$$x_{10} = \frac{1}{C_1^r} \quad x_{11} = \frac{1}{C_w R_w} \quad (20)$$

$$x_{12} = \frac{1}{C_{51}^w R_{51_1}} \quad x_{13} = \frac{1}{C_{51}^w R_{51_5}} \quad (21)$$

$$x_{14} = \frac{\alpha}{C_{51}^w} \quad x_{15} = \frac{1}{R_{15}^{win}} \quad (22)$$

As it can be seen in the continuous state space form, rate of change of these augmented states is equal to zero. We later add a low-magnitude *fictitious noise* to the dynamics of parameters to allow slow changes in the values of parameters over time.

$$\begin{aligned} \dot{x}_1 = & (x_6 - x_7 - x_8 - x_9 - x_{10}x_{15} - x_{10}u_2c_a)x_1 \\ & + x_6x_2 + x_7x_3 + x_8x_4 + x_9x_5 + (c_a u_1 u_2 \\ & + T_5 x_{15} + A_{win} \tau Q_{rad} + \dot{Q}_{int}) \cdot x_{10} \end{aligned} \quad (23)$$

$$\dot{x}_2 = (x_1 - 2x_2 + T_2) \cdot x_{11} \quad (24)$$

$$\dot{x}_3 = (x_1 - 2x_3 + T_3) \cdot x_{11} \quad (25)$$

$$\dot{x}_4 = (x_1 - 2x_4 + T_4) \cdot x_{11} \quad (26)$$

$$\dot{x}_5 = x_1 x_{12} - (x_{12} + x_{13}) x_5 + T_5 x_{13} + A^{w51} x_{14} Q_{rad} \quad (27)$$

$$\dot{x}_i = 0 \quad \forall i = 6, 7, \dots, 15. \quad (28)$$

where u is the input vector:

$$u = \begin{bmatrix} T_{s1} \\ \dot{m}_{r1} \end{bmatrix} \quad (29)$$

In summary, we express the dynamics of the system using

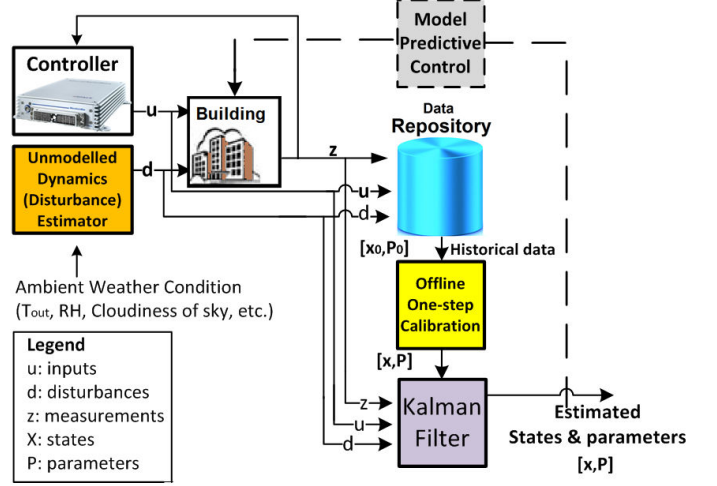


Figure 2. Architecture of the proposed PAB model with its components. Note that the dashed line proposes the use of this technique to provide updated model parameters to the more sophisticated control techniques, such as MPC. However, design of MPC is not the focus of this paper.

state space model below:

$$\begin{aligned} x_k &= f(x_{k-1}, u_{k-1}, d_{k-1}, w_{k-1}) \\ z_k &= h(x_k) + v_k \end{aligned} \quad (30)$$

where w_k and v_k are the process and measurement noise and are assumed to be zero mean multivariate Gaussian process with covariance W_k and V_k , (i.e. $w_k \sim N(0, W_k)$ and $v_k \sim N(0, V_k)$), respectively.

3 Combined State-Parameter Estimation

In order to estimate the unknown parameters of the system we augment the states of the system with a vector p_k which stores the parameters of the system, with a time evolution dynamics of $p_{k+1} = p_k$, as explained in Section 2. Nonlinear estimation algorithms can then be exploited to simultaneously estimate the states and the parameters of the system. Here we exploit the extended Kalman filter (EKF) and unscented Kalman filter (UKF) techniques. Simulation results are compared in Section 5. The architecture of the proposed Parameter-Adaptive Building (PAB) model is shown in Fig. 2.

3.1 Extended Kalman Filter

In the EKF, the state transition and observation models need not be linear functions of the state but may instead be differentiable functions. The Kalman filter algorithm consists of two steps – *prediction* followed by *update*. The states of the system are approximated by a Gaussian random variable. In the prediction step, the filter propagates the *a-priori* state estimate through the nonlinear state update equation from time step $k - 1$

to the current time step k , and the state estimation error covariance is propagated through the linearized approximation of the state equations to compute the *a-priori* state estimation error covariance. In the *update* step, the *a-posteriori* state estimate and state estimation error covariance are computed.

With the stochastic state update equation given in (30), and the following notations

$$\hat{x}_{k|k-1} = \mathbb{E}[x_k | z_0, z_1, \dots, z_{k-1}] \quad (31)$$

$$\hat{x}_{k|k} = \mathbb{E}[x_k | z_0, z_1, \dots, z_k] \quad (32)$$

$$P_{k|k-1} = \mathbb{E}[(x_k - \hat{x}_{k|k-1})(x_k - \hat{x}_{k|k-1})^T | z_0, z_1, \dots, z_{k-1}] \quad (33)$$

$$P_{k|k} = \mathbb{E}[(x_k - \hat{x}_{k|k})(x_k - \hat{x}_{k|k})^T | z_0, z_1, \dots, z_k] \quad (34)$$

where $\mathbb{E}[x|y]$ represents mean of variable x , given measurement y . Each iteration of the EKF is summarized as follows:

Extended Kalman Filter Algorithm

Prediction:

A-priori state estimate: $\hat{x}_{k|k-1} = f(\hat{x}_{k-1|k-1}, u_{k-1}, d_{k-1}, 0)$

State transition and observation matrices:

$$F_{k-1} = \left. \frac{\partial f}{\partial x} \right|_{\hat{x}_{k-1|k-1}, u_{k-1}} \quad H_k = \left. \frac{\partial h}{\partial x} \right|_{\hat{x}_{k|k-1}}$$

A-priori state estimation error covariance:

$$P_{k|k-1} = F_{k-1} P_{k-1|k-1} F_{k-1}^T + W_{k-1}$$

Update:

A-priori output estimation error: $\tilde{y}_k = z_k - h(\hat{x}_{k|k-1})$

Innovation or residual covariance: $S_k = H_k P_{k|k-1} H_k^T + V_k$

Near-optimal Kalman gain: $K_k = P_{k|k-1} H_k^T S_k^{-1}$

A-posteriori state estimate: $\hat{x}_{k|k} = \hat{x}_{k|k-1} + K_k \tilde{y}_k$

A-posteriori state estimation error covariance: $P_{k|k} = (I - K_k H_k) P_{k|k-1}$

3.2 Unscented Kalman Filter

A nonlinear KF that shows promise as an improvement over the EKF is the unscented Kalman filter (UKF). The basic premise behind the UKF is that it is easier to approximate a Gaussian distribution than to approximate an arbitrary nonlinear function. The UKF addresses the approximation issues of the EKF. Instead of using Jacobian matrix, UKF uses a deterministic sampling approach to capture the mean and covariance estimates with a minimal set of sample points [13]. As with the EKF, we present an algorithmic description of the UKF, omitting some theoretical considerations. More details can be found in [14, 15].

The state distribution is represented by a Gaussian random variable (GRV), but is now specified using a minimal set of care-

fully chosen sample points. These sample points completely capture the true mean and covariance of the GRV, and when propagating through the true nonlinear system, capture the posterior mean and covariance accurately to the 3rd order (Taylor series expansion) for any nonlinearity. Unscented Transformation (UT) is a method used for calculating the statistics of a random variable which undergoes a nonlinear transformation [14]. We conduct the following initialization:

$$\hat{x}_0 = \mathbb{E}[x_0] \quad (35)$$

$$P_0 = \mathbb{E}[(x_0 - \hat{x}_0)(x_0 - \hat{x}_0)^T] \quad (36)$$

Each step of the UKF can be summarized as follows:

Unscented Kalman Filter Algorithm

Prediction:

Calculate sigma points:

$$\mathcal{X}_{k-1} = [\hat{x}_{k-1} \quad \hat{x}_{k-1} + \gamma\sqrt{P_{k-1}} \quad \hat{x}_{k-1} - \gamma\sqrt{P_{k-1}}]$$

Propagate each column of \mathcal{X}_{k-1} through time:

$$(\mathcal{X}_k)_i = f((\mathcal{X}_{k-1})_i) \quad i = 0, 1, \dots, 2L$$

A-priori state estimate: $\hat{x}_k^- = \sum_{i=0}^{2L} W_i^{(m)} (\mathcal{X}_k)_i$

A-priori error covariance:

$$P_k^- = \sum_{i=0}^{2L} W_i^{(c)} [(\mathcal{X}_k)_i - \hat{x}_k^-][(\mathcal{X}_k)_i - \hat{x}_k^-]^T + Q_k$$

Update:

Measurement estimate: $(Z_k)_i = h((\mathcal{X}_k)_i) \quad i = 0, \dots, 2L$

$$\hat{z}_k^- = \sum_{i=0}^{2L} W_i^{(m)} (Z_k)_i$$

A-posteriori state estimate: $\hat{x}_k = \hat{x}_k^- + K_k (z_k - \hat{z}_k^-)$

where: $K_k = P_k^- P_{\hat{z}_k^-}^{-1}$

A-posteriori estimate of the error covariance: $P_k = P_k^- - K_k P_{\hat{z}_k^-} K_k^T$

where:

$$P_{\hat{x}_k \hat{z}_k} = W_i^{(c)} [(\mathcal{X}_k)_i - \hat{x}_k^-][(\mathcal{Z}_k)_i - \hat{z}_k^-]^T$$

$$P_{\hat{z}_k \hat{z}_k} = \sum_{i=0}^{2L} W_i^{(c)} [(\mathcal{Z}_k)_i - \hat{z}_k^-][(\mathcal{Z}_k)_i - \hat{z}_k^-]^T + R_k$$

where \hat{x}^- denotes a-priori estimate of x . $\gamma = \sqrt{(L + \lambda)}$, and $\lambda = \alpha^2(L + \delta) - L$ are the composite scaling parameters. α is a scaling parameter that determines the spread of the sigma

points around \hat{x} , and is usually set to a small positive value (e.g. $1e-4 \leq \alpha \leq 1$). δ is a secondary scaling parameter which is usually set to 0 or $3-L$ [15]. Q_k is the process error covariance matrix and R_k is the measurement noise covariance matrix. $W_i^{(m)}$ and $W_i^{(c)}$ weights are defined by:

$$W_i^{(m)} = \begin{cases} \frac{\lambda}{(L+\lambda)}, & \text{if } i = 0 \\ \frac{1}{2(L+\lambda)}, & \text{if } i = 1, 2, \dots, 2L \end{cases} \quad (37)$$

and

$$W_i^{(c)} = \begin{cases} \frac{\lambda}{L+\lambda} + (1 - \alpha^2 + \beta), & \text{if } i = 0 \\ \frac{1}{2(L+\lambda)}, & \text{if } i = 1, 2, \dots, 2L \end{cases} \quad (38)$$

where β is a parameter used to incorporate the prior knowledge of the distribution of x . We use $\beta = 2$ which is optimal for Gaussian distributions [16].

4 Test-Bed and Historical Data

The model studied in this paper is a model for an office with a simple structure in the Lakeshore building at Michigan Technological University. This room is surrounded by two rooms and a corridor in the building and connected to the outdoor area with a thick concrete wall and two south-oriented double-layered windows. Each room is equipped with temperature and humidity sensors (Uni-curve Type II) with the temperature accuracy of $\pm 0.2^\circ\text{C}$. We have installed a temperature data logger with accuracy of $\pm 0.8^\circ\text{C}$ inside the main room to estimate measurement errors. Temperature readings from these two sensors are shown in Fig. 3. We follow the methodology proposed in [17] to find the temperature measurement accuracy, which is obtained to be $\pm 0.82^\circ\text{C}$, and is used in the EKF and UKF algorithms. There are also some other sensors throughout the university to measure and record the outdoor temperature. All the sensors' measurements for the building network are available through the Building Management System (BMS).

The HVAC system in the building uses Water-Source Heat-Pumps (WSHP) to maintain required energy for heating purposes. Each unit in this system provides heating for an individual zone. Therefore, a unit operates when heating is required for its zone and the set point can be defined independently based on the functionality of each zone. The HVAC system uses an on-off controller to provide a desired temperature for each zone. When the temperature goes below a set point by 0.28°C (0.5°F), the heating system is switched on until it reaches the adjusted set point. To maintain standard internal air quality (IAQ) for each zone, a supply fan with a constant mass flow rate of 0.52 (kg/s) works between 4AM to 6 PM (except for holidays). Zone temperatures are measured with a sampling period of 60 seconds.

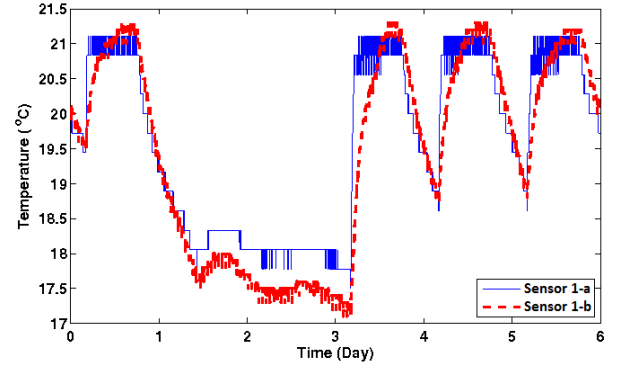


Figure 3. Data logger and BMS sensor temperature readings

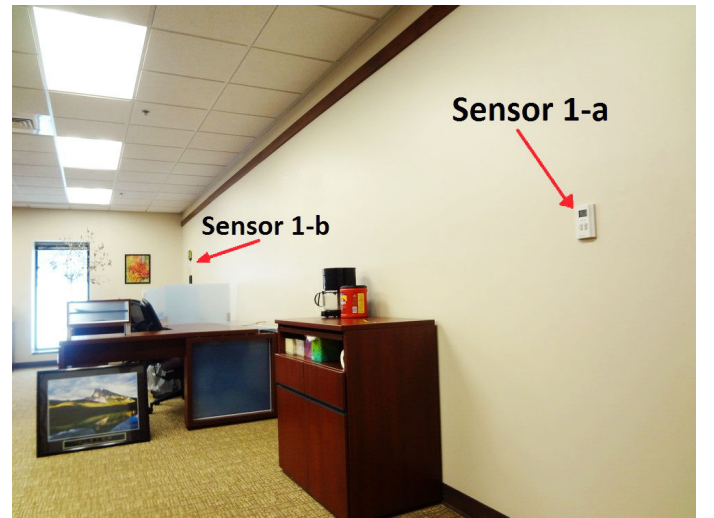


Figure 4. Location of the temperature sensors in the test-bed

5 Results

The test-bed from previous section was used to collect measurements from January 11 to January 24, 2013. To remove noise from the temperature measurements, a second order Butterworth lowpass filter with cutoff frequency of 0.001 Hz was used.

We implement both the EKF and the UKF and present the results of the simulations. Fig. 5 shows the temperatures of the neighboring zones and the outside temperature which act as disturbance to the model. Fig. 6 depicts the model inputs including the air mass flow rate and the supply air temperature. In order to obtain the best initial parameter values for the Kalman filter algorithms, we first perform a (static) parameter identification on the historical data. We consider the first part of the data as *training data set* (shown in red in Fig. 7), and obtain the best parameters that minimize the error between the simulation and the measurement in least square sense. The result of this step is used to simulate the temperature evolution of the room air for the next three days (shown in black in Fig. 7). Due to time-varying parameters and disturbance to the model, it is difficult to find a set

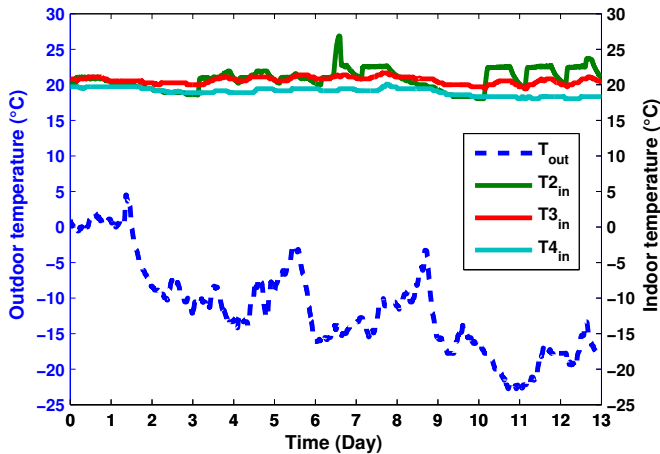


Figure 5. Disturbances to the PAB model.

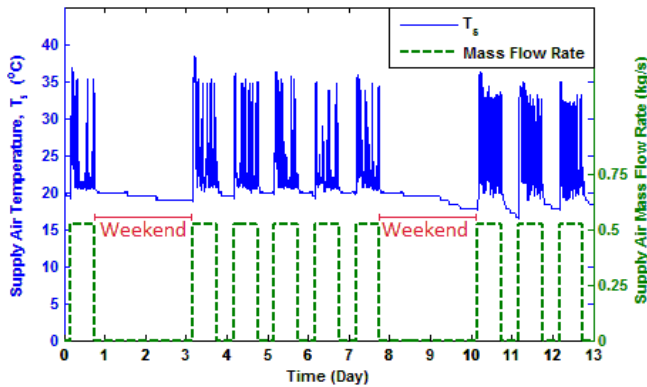


Figure 6. Inputs to the PAB model.

of parameters for the model which results in good temperature tracking for all days, and hence, as shown in Fig. 7, the results of simulations for the following days in the testing data set is even worse.

The obtained initial parameters from the off-line calibration step is used as initial point for the EKF and UKF algorithms.

5.1 EKF Results

Temperature estimation of room and walls, using EKF are depicted in Fig. 8 and Fig. 9. The results show that although the initial parameters from the training data set is not necessarily optimal for future days, the PAB model manages to tune the parameters and leads to very good temperature tracking (Fig. 8).

Fig. 10 shows the evolution of parameters over time. In this case, EKF only temporarily changes the value of parameters when necessary, but the steady state values of the parameters are close to the initial values obtained from the one shot parameter identification using historical data.

Note that although the room temperature estimations are

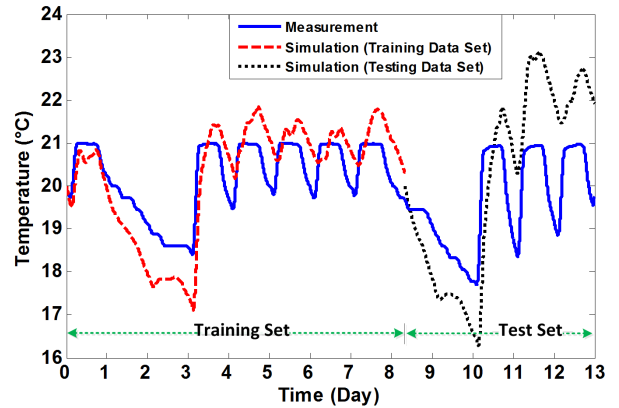


Figure 7. The first set of data (shown in red) is the training data. We identify the parameters in a one shot optimization by minimizing the l_2 norm of the error between simulation and measurement data. Then we used the obtained parameters from the training data set to predict the temperature evolution for the next days (shown in black).

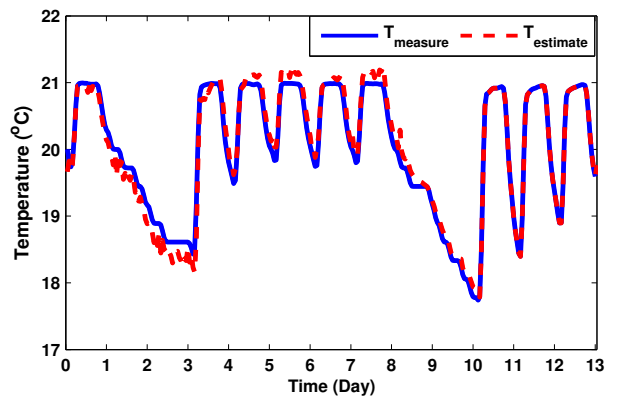


Figure 8. Estimated and measured room temperature using EKF.

close to the actual room temperature, the temperature of walls are not realistic in the EKF case. Hence we also try UKF and report the results in what follows.

5.2 UKF Results

We follow the same steps to first acquire the best initial parameters by an off-line optimization and then use the obtained parameters as initial value for UKF. The temperature estimation of room and walls, using UKF are depicted in Fig. 11 and Fig. 12. The evolution of parameters over time is shown in Fig. 13. In this case, contrary to the EKF case, the parameters evolve over time and the steady state values are not necessarily close to the initial points.

Note that the first part of the estimation of wall temperature by UKF leads to overshoot in the wall temperature, however, this overshoot is quickly recovered as UKF uses more data to tune the parameters more accurately. Overall, the UKF outperforms

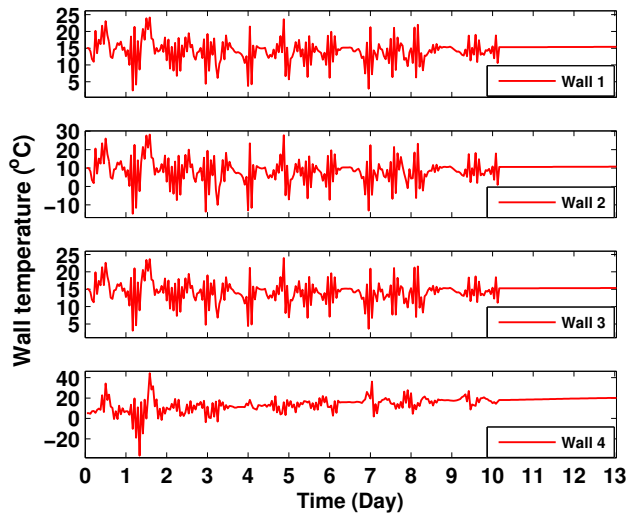


Figure 9. Estimated temperature of walls using EKF.

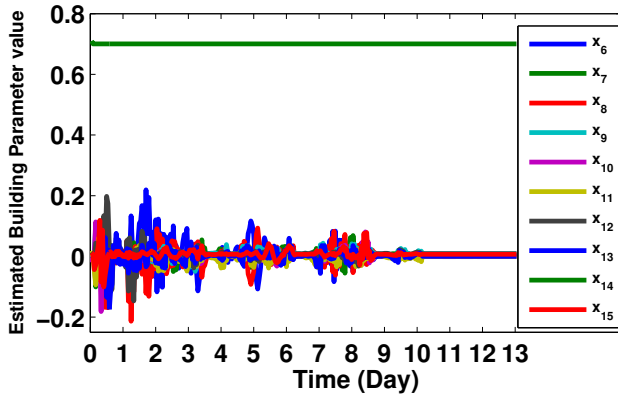


Figure 10. Estimated parameters of the system using EKF.

the EKF in providing an accurate PAB mode because: 1) the estimation of room temperature is more accurate. 2) the estimated temperatures of walls are more realistic in the UKF case. High frequency oscillations in the wall temperature estimation of EKF is observed (Fig. 9), but these fast temperature oscillations of walls are not realistic due to the large heat capacitance of the walls. The dynamics of wall temperatures determined by the UKF algorithm seem intuitive and correct, given the slower dynamics *i.e.* small frequency oscillations.

6 Summary and Conclusion

We presented a framework for simultaneous state estimation and parameter identification of building predictive models. To develop a Parameter-Adaptive Building (PAB) model, we first constructed a nonlinear state space model by augmenting the parameters of the system into the state vector. We exploited the

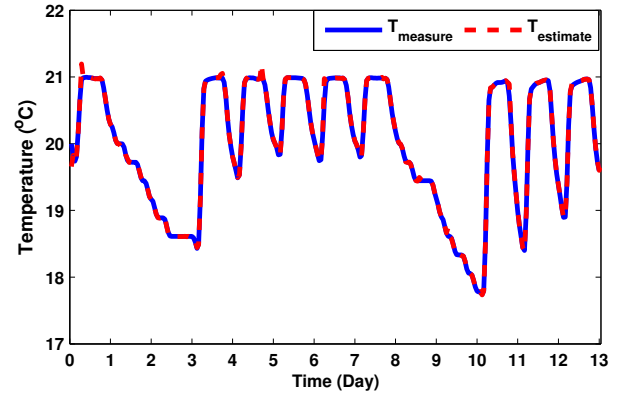


Figure 11. Estimated and filtered temperature of room using UKF.

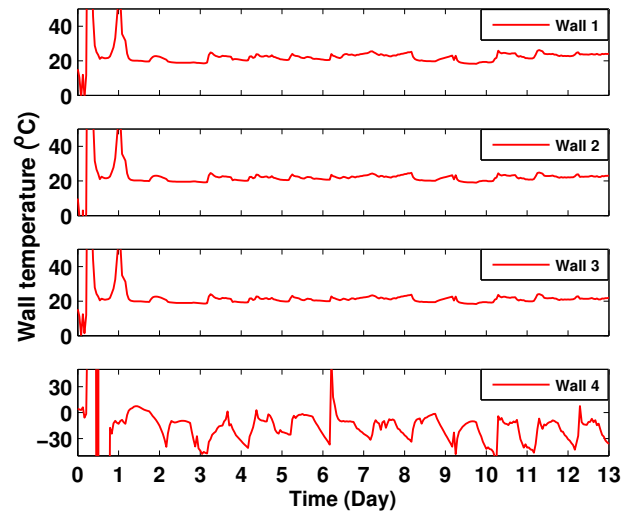


Figure 12. Estimated temperature of walls using UKF. We have zoomed the figures to focus on the more steady estimates of the walls rather than the first part transient behavior.

similarities in the physical properties such as wall materials and thicknesses in the building under study, and reduced the number of independent parameters in the building model. We then utilized the developed model in the extended Kalman filter (EKF) and unscented Kalman filter (UKF) to simultaneously estimate all the states of the dynamic model and continuously and in an *online* fashion tune the parameters of the model. The results of testing both EKF and UKF showed that UKF outperforms EKF as it yields a more accurate room temperature estimation as well as more realistic estimations of wall temperatures. The PAB model from this work can easily be extended to cover an entire building. In future work, we plan to apply the PAB model for model predictive control of buildings.

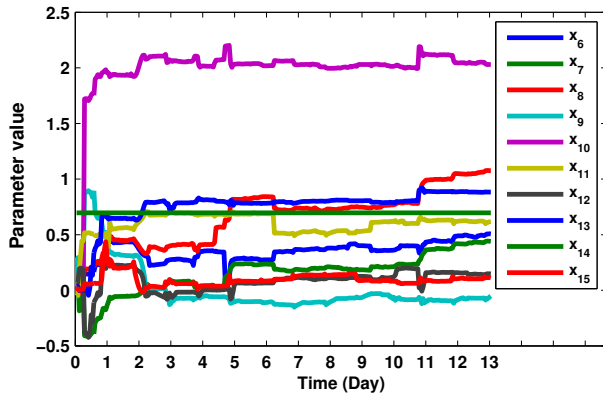


Figure 13. Estimated parameters of the system using UKF.

ACKNOWLEDGMENT

Special thanks to Mr. Gregory Kaurala (MTU Energy Management Assistant) for his help in collecting the experimental data and his technical review and advice. Mehdi Maasoumy is funded by the Republic of Singapore's National Research Foundation through a grant to the Berkeley Education Alliance for Research in Singapore (BEARS) for the Singapore-Berkeley Building Efficiency and Sustainability in the Tropics (SinBerBEST) Program. BEARS has been established by the University of California, Berkeley as a center for intellectual excellence in research and education in Singapore. Alberto Sangiovanni Vincentelli is supported in part by the TerraSwarm Research Center, one of six centers administered by the STARnet phase of the Focus Center Research Program (FCRP), a Semiconductor Research Corporation program sponsored by MARCO and DARPA.

REFERENCES

- [1] Building Energy Data Book of DOE (2013, Jan). [Online]. Available: <http://buildingsdatabook.eren.doe.gov/>
- [2] M. Maasoumy and A. Sangiovanni-Vincentelli, "Total and Peak Energy Consumption Minimization of Building HVAC Systems using Model Predictive Control," *IEEE Design and Test of Computers*, 2012.
- [3] S. Prvara, J. Cigler, Z. Va, F. Oldewurtel, C. Sagerschnig, and E. ekov, "Building Modeling as a Crucial Part for Building Predictive Control," *Energy and Buildings*, vol. 56, pp. 8 – 22, 2013. [Online]. Available: <http://www.sciencedirect.com/science/article/pii/S0378778812005336>
- [4] M. Maasoumy Haghighi, "Modeling and Optimal Control Algorithm Design for HVAC Systems in Energy Efficient Buildings," Master's thesis, EECS Department, University of California, Berkeley, Feb 2011. [Online]. Available: <http://www.eecs.berkeley.edu/Pubs/TechRpts/2011/EECS-2011-12.html>
- [5] M. Maasoumy, A. Pinto, and A. Sangiovanni-Vincentelli, "Model-Based Hierarchical Optimal Control Design for HVAC Systems," in *Dynamic System Control Conference (DSCC)*. ASME, 2011.
- [6] F. Oldewurtel, A. Parisio, C. Jones, M. Morari, D. Gyalistras, M. Gwerder, V. Stauch, B. Lehmann, and K. Wirth, "Energy Efficient Building Climate Control using Stochastic Model Predictive Control and Weather Predictions," in *American Control Conference (ACC)*. IEEE, 2010, pp. 5100–5105.
- [7] C. Agbi, Z. Song, and B. Krogh, "Parameter Identifiability for Multi-Zone Building Models," in *IEEE 51st Annual Conference on Decision and Control (CDC)*, 2012, pp. 6951–6956.
- [8] G. L. Plett, "Sigma-Point Kalman Filtering for Battery Management Systems of LiPB-Based HEV Battery Packs: Part 2: Simultaneous State and Parameter Estimation," *Journal of Power Sources*, vol. 161, no. 2, pp. 1369–1384, 2006.
- [9] H. Moradkhani, S. Sorooshian, H. V. Gupta, and P. R. Houser, "Dual State-Parameter Estimation of Hydrological Models Using Ensemble Kalman Filter," *Advances in Water Resources*, vol. 28, no. 2, pp. 135–147, 2005.
- [10] M. Rafiee, A. Tinka, J. Thai, and A. M. Bayen, "Combined state-parameter estimation for shallow water equations," in *American Control Conference (ACC)*. IEEE, 2011, pp. 1333–1339.
- [11] M. Goforth, G. Gilcrest, and J. Sirianni, "Cloud Effect on Thermal Downwelling Sky Radiance," *Proc. SPIE, Society of Photo-Optical Instrumentation Engineers*, vol. 4710–27, no. 1, pp. pp 203–213, 2002.
- [12] National Renewable Energy Laboratory (2013, Jan). [Online]. Available: <http://www.nrel.gov/>
- [13] E. Wan and R. Van Der Merwe, "The Unscented Kalman Filter for Nonlinear Estimation," in *Adaptive Systems for Signal Processing, Communications, and Control Symposium. AS-SPCC*. IEEE, 2000, pp. 153–158.
- [14] S. Julier and J. Uhlmann, "A New Extension of the Kalman Filter to Nonlinear Systems," in *Int. Symp. Aerospace/Defense Sensing, Simul. and Controls*, vol. 3. Spie Bellingham, WA, 1997, p. 26.
- [15] D.-W. H. Julier S.J., Uhlmann J.K., "A New Approach for Filtering Nonlinear Systems," in *Proceedings of the American Control Conference*, vol. 3. IEEE, 1995, pp. 1628–1632.
- [16] E. Wan and R. Van Der Merwe, "The Unscented Kalman Filter," *Kalman Filtering and Neural Networks*, pp. 221–280, 2001.
- [17] M. Maasoumy, Q. Zhu, C. Li, F. Meggers, and A. Sangiovanni-Vincentelli, "Co-Design of Control Algorithm and Embedded Platform for HVAC Systems," in *The 4th ACM/IEEE International Conference on Cyber-Physical Systems (ICCPS 2013)*, Philadelphia, USA, Apr. 2013.